

Received XXXX

(www.interscience.wiley.com) DOI: 10.1002/sim.0000

The development of an early warning system for climate-sensitive disease risk with a focus on dengue epidemics in Brazil

Rachel Lowe^{a*}, Trevor C. Bailey^b, David B. Stephenson^b, Tim E. Jupp^b, Richard J. Graham^c, Christovam Barcellos^d and Marilia Sá Carvalho^d

Previous studies have demonstrated statistically significant associations between disease and climate variations, highlighting the potential for developing climate-based epidemic early warning systems. However, limitations to such studies include failure to allow for non-climatic confounding factors, limited geographical/temporal resolution, or lack of evaluation of predictive validity. Here, we consider such issues in the context of dengue fever in South East Brazil, where dengue epidemics impact heavily on Brazilian public health services. A spatio-temporal generalised linear mixed model (GLMM) is developed, including both climate and non-climate covariates. Overdispersion and unobserved confounding factors are accounted for via a Negative Binomial formulation and inclusion of both spatial and temporal random effects. Model parameters are estimated in a Bayesian framework to allow full posterior predictive distributions for disease risk to be derived in time and space. Detailed probabilistic forecasts can then be issued for any pre-defined 'alert' thresholds, allowing probabilistic early warnings for dengue epidemics to be made. Using this approach with the criterion 'greater than a 50% chance of exceeding 300 cases per 100,000 inhabitants', successful epidemic alerts would have been issued for 81% of the 54 regions that experienced epidemic dengue incidence rates in South East Brazil, during the major 2008 epidemic. Use of seasonal climate forecasts in this model allows predictions to be made several months ahead of an impending epidemic. We argue that the general modelling framework, described here in the context of dengue in Brazil, is potentially valuable in similar applications, both outside of Brazil and for other climate-sensitive diseases. Copyright © 0000 John Wiley & Sons, Ltd.

Keywords: Climate; dengue; early warning systems; random effects; spatio-temporal modelling

^a International Centre for Theoretical Physics, I - 34151, Trieste, Italy

^b University of Exeter, EX4 4QF, UK

^b Met Office Hadley Centre, Exeter, EX1 3PB, UK

^d Oswaldo Cruz Foundation, Rio de Janeiro, CEP 21045-900, Brazil

* Correspondence to: Rachel Lowe, International Centre for Theoretical Physics, I - 34151, Trieste, Italy, Tel: +39 040 2240 360, Fax: +39 040 2240 449, E-mail: rlowe@ictp.it

Contract/grant sponsor: This work was supported by the EUROBRISA network project (F/00 144/AT) kindly funded by the Leverhulme Trust.

1. Introduction

The transmission of many infectious diseases is often influenced by weather and climate variability, particularly for those spread by arthropod vectors such as malaria and dengue [1]. Some vector-borne diseases demonstrate seasonal patterns and display inter-annual variability which can partly be explained by meteorological factors [2]. Therefore, climate information could potentially be valuable in early warning systems for epidemic-prone diseases, to provide public health decision makers and the general public with as much advance notice as possible about the likelihood of an epidemic. This would allow the implementation of timely preventative measures. Such early warning systems require statistical and/or biological models which incorporate the impact of climate variables on disease transmission. Due to time lags involved in the climate-disease transmission system, lagged observed climate variables could provide some predictive lead for forecasting disease epidemics. This lead time can be extended by using forecast climate in disease prediction models. This is a topic of particular interest given the increasing international scientific effort being invested in refinement of seasonal forecasting models, and on-line access to such predictions (e.g. <http://eurobrisa.cptec.inpe.br/>).

Recent epidemiological studies have demonstrated statistically significant associations between climate variations and various infectious diseases (for a review see [3]), and have highlighted the potential for developing climate-based early warning systems (e.g. [4]). However, developing statistical models based on past empirical data that adequately capture associations between climate-sensitive disease and climatic factors can be problematic. To measure how much variation in disease risk can be attributed to climatic factors, non-climatic confounding factors must also be carefully considered to avoid drawing misleading conclusions in estimating climate-disease associations. Some relevant information can be obtained from census data and other routinely collected sources, but data on many localised confounding factors is scarce on a scale suitable to address the needs of public health services. Therefore, statistical climate-disease models need to make due allowance for latent structure relating to unobserved temporal and/or spatial confounding factors.

Another major barrier to developing such models is the relatively short length of available time series of good quality disease data and the lack of spatial resolution at the sub-national level in such data sets. Epidemics are often sudden and unexpected, and prevention and control strategies need to be accurately targeted in both time and space if they are to stand a chance of being effective [5]. When sufficient space-time data is available, it is usually a mixture of multi-scaled observations, differentially aggregated or averaged in time and space. This implies the need to allow for complex correlation structures in the model formulation and possibly multi-level (hierarchical) structure. Further complications can also arise when disease-climate relationships exhibit 'threshold' or 'extreme' dependencies, rather than average behaviour.

An important further requirement is the evaluation of statistical disease models. A proper assessment of predictive performance is required along with an evaluation of the practical application of the model in a public health context. The tendency of a disease forecasting system to issue false alarms (issuing an epidemic warning when no epidemic is later observed) or to miss an epidemic can have serious consequences. Not only in terms of morbidity and mortality, but also in terms of economic cost and the willingness of the public to rely on subsequent warnings [6]. In all cases, model performance should be validated using out-of-sample data [5].

As an alternative to statistical models, mathematical process models are increasingly being applied to interpret and predict the future incidence and control of infectious diseases (e.g. [7, 8, 9]). Whereas statistical models are driven by data and use empirical (or 'descriptive') relationships between the disease and climate variables, process-based models use largely deterministic differential equations to represent the dynamical evolution of the disease lifecycle and incorporate climate influences as parameters. As process models are based on underlying physical and biological processes, some have argued that they are potentially more powerful than their purely data driven, 'descriptive' statistical counterparts. They can, for example, be applied to regions where reliable data is lacking, or to predict future disease behaviour based on postulated climate scenarios. However, in practice such models are often limited by a lack of full understanding of the biological mechanisms involved, or omission of significant aspects of the vector or parasite lifecycle (due to the lack of information in the literature) and also by the availability of data for model input and model validation [10]. Parameter

settings are often selected according to a limited number of site specific field or laboratory studies which may not be applicable to different regions.

Notwithstanding some of the potential theoretical advantages of process-based models, we argue that ‘descriptive’ statistical climate-disease models based on past empirical data provide a valuable, viable and effective approach to developing practical epidemic early warning systems. Such models have the advantage of being able to incorporate a sufficiently wide range of both climatic and non-climatic (confounding) explanatory variables [11] and make best use of routinely available data. We also show that judicious use of sufficiently sophisticated modern statistical modelling methods can address or reduce the various potential difficulties that may be associated with developing such models, i.e. unobserved confounding factors, complex correlation structures, proper evaluation of predictive power, etc.

We illustrate this in the context of developing an early warning system for dengue fever in South East Brazil. Brazil is used as a case study to show how a well-specified statistical model can be developed, which is capable of providing probabilistic forecasts and practically useful early warnings of future and geographically specific risk of dengue epidemics. In the 21st century, Brazil became the country with the most reported cases of dengue fever in the world. More than three million cases were reported from 2000 to 2005 [12], representing 78% of all cases reported in the Americas and 61% of all cases reported to the World Health Organization (WHO). Large areas of Brazil have highly favourable climate for the proliferation of *Aedes aegypti* mosquitoes and dozens of metropolises with high human population densities living in substandard conditions with deficient sanitation services [12]. Brazil also has some of the world's best laboratory-based surveillance capabilities for dengue/dengue haemorrhagic fever [13]. However, data from this surveillance system is not routinely nor effectively exploited in any early warning system to predict epidemics. Therefore, Brazil serves as an excellent ‘test bed’ for which to develop a climate-based early warning system for dengue epidemics. We focus our analysis on the South East region of Brazil where dengue is most prevalent and there are a large number of densely populated urban centres which could benefit from a climate informed dengue early warning system. This is also the region of Brazil where previous work has reported climate influences to be significantly associated with observed spatio-temporal variability in dengue risk (see [14]).

Although the specific model details and results in subsequent sections relate to our Brazilian case study on dengue, we believe that the general methodological framework and considerations we describe are more widely applicable, both outside of Brazil and to climate sensitive diseases other than dengue.

2. Dengue

Dengue fever is currently one of the most important emerging tropical diseases in the world in terms of morbidity and mortality [15, 16]. It is an acute mosquito-borne viral disease characterised by fever, headache, severe muscle and joint pains (hence commonly referred to as ‘break-bone fever’), rash, nausea, and vomiting [17]. Most dengue infections do not result in death, but a small portion develop into the more serious and potentially deadly illness dengue hemorrhagic fever/dengue shock syndrome. This is characterized by spontaneous hemorrhage, increased permeability of the blood vessels and circulatory failure, leading to shock. Fatality rates in untreated dengue hemorrhagic fever/dengue shock syndrome can be as high as 50% [18]. Global incidence of dengue has grown dramatically in recent decades and according to the WHO, about two fifths of the world's population are now at risk, with an estimated 50 million dengue infections worldwide every year. Dengue is caused by any of four closely related dengue virus strains or serotypes (DENV-1,2,3 and 4), belonging to the family Flaviviridae [19]. Infection with one serotype provides life-long immunity against further infection from that same serotype but no protection against the other serotypes. In fact, it has been hypothesised that sequential infections with other serotypes increases the risk of more severe manifestations including dengue hemorrhagic fever and dengue shock syndrome [20].

The vector responsible for major dengue epidemics is the domestic, container breeding *Aedes Aegypti* mosquito [21].

The resurgence of epidemic dengue fever and the emergence of dengue hemorrhagic fever in the last few decades have been closely tied with population growth, urbanisation and air travel [22, 23]. Dengue incidence is usually associated with warmer, more humid weather. Rainfall may influence dengue incidence through the filling of containers out in the open (e.g. old tyres), which create potential breeding sites for the mosquito, while the subsequent cycle also depends on temperature and humidity [24]. For a dengue epidemic to occur, a large number of mosquitoes are required along with many people with no immunity to one of the four dengue serotypes and an opportunity for the two to interact. The many potential drivers of dengue, both extrinsic, such as climate, and intrinsic, such as population immunity are often difficult to disentangle. This presents a challenge for modelling of dengue risk in space and time.

Despite significant progress in vaccine development [25, 26], there is no tested and approved vaccine to protect against dengue. Therefore, disease control and prevention have mainly focused on vector control activities and surveillance [27, 12]. Although there is no specific treatment for dengue, appropriate medical care frequently saves the lives of patients with the more serious dengue haemorrhagic fever. The current dengue surveillance system in Brazil relies on observing early cases of dengue in December/January to estimate epidemic potential later in the austral summer (see [14]). However, this provides neither quantitative estimates nor a long predictive lead time. The greater the lead time available for forecasting disease risk, the greater the opportunity for effective disease risk intervention, such as preparing health care services for increased numbers of dengue patients and educating populations to eliminate mosquito breeding sites. As the lead time of a dengue prediction model could potentially be extended by using climate, or even forecasts of the climate, the development and evaluation of a climate informed dengue early warning system for Brazil is a worthwhile endeavour.

3. Data

3.1. Dengue, demographic and cartographic data

Dengue fever data (counts of notified cases per calendar month) from January 2001 - December 2009 were obtained at municipality level from DATASUS (<http://dtr2004.saude.gov.br/sinanweb/novo/>). The data set includes all notified dengue cases from hospitals and clinic doctors from both the private and public health system. Individual data are locally entered into the electronic information system and subsequently transmitted to state and national levels [27]. Cases are laboratory confirmed where possible, or otherwise based on syndromic definition. A network of laboratories, capable of diagnosing dengue infections, has been implemented in all Brazilian states. The network is responsible for confirmation of cases to support epidemiological surveillance [28]. However, this network is not accessible to all municipalities within the states. To address this issue, dengue counts were aggregated to the lower resolution microregion level, where a microregion typically consists of one large city and several smaller municipalities (there are 160 such defined microregions in South East Brazil). This alleviates problems of misreporting due to variation in availability of health services/epidemiological facilities at the municipality level.

The Brazilian Ministry of Health define yearly dengue incidence rates (DIR) as the number of new dengue cases per 100,000 inhabitants for a geographical area. In order to calculate incidence rates using the dengue count dataset described above, yearly population estimates for Brazilian microregions from 2001-2009 were obtained from the Brazilian Institute for Geography and Statistics (IBGE) (<http://www.ibge.gov.br/>). These estimates are based on the 2000 census and take into account changing demographic components such as births, mortality and migration. Although the models in subsequent sections are specified for counts of dengue cases, results in this paper are reported in terms of DIR for ease of interpretation.

Figure 1a shows the time series of DIR for the 2001-2009 period for South East Brazil. Two major epidemics occurred in the late austral summer of 2002 and 2008, while considerably fewer dengue cases were reported in 2004 and 2005. Figure 1b illustrates the spatial distribution of DIR according to the three risk categories; high (more than 300 cases per 100,000), medium (between 100 and 300 cases per 100,000) and low incidence (less than 100 cases per 100,000).

National cartographic data such as altitude and area were obtained from IBGE. Census data for microregions related to levels of urbanisation were obtained from an aggregated database, SIDRA (<http://www.sidra.ibge.gov.br>) maintained by IBGE and included variables such as the percentage of urban population, households with at least one bathroom, refuse collection and water supply provided by a network.

3.2. Climate data

Observed gridded ($2.5^\circ \times 2.5^\circ$ latitude-longitude grid) average monthly rate of precipitation data were obtained from the Global Precipitation Climatology Project (GPCP) [29]. The dataset is a combination of gauge observations with satellite estimates from 1979 to present. Reanalysis gridded ($2.5^\circ \times 2.5^\circ$ latitude-longitude grid) monthly mean surface air temperature data were obtained from the NCEP/NCAR Reanalysis. The NCEP/NCAR Reanalysis project uses a state-of-the-art analysis/forecast system to perform data assimilation using past data from 1948 to the present [30]. Precipitation and temperature data from both the GPCP combined rain gauge-satellite dataset and the reanalysis project were extracted for the period 2000–2009 and will be referred to as ‘observed’ climate variables in the remainder of this paper.

A time series of the Oceanic Niño Index (ONI), defined as the 3-month running mean of sea surface temperature (SST) anomalies in the Niño 3.4 region (120°W – 170°W and 5°S – 5°N), based on the 1971–2000 base period, was obtained from the NOAA Climate Prediction Center (CPC) (http://www.cpc.noaa.gov/products/analysis_monitoring/ensostuff/ensoyears.shtml). Warm (El Niño) and cold (La Niña) episodes of the El Niño Southern Oscillation (see [31]) are based on a threshold of $\pm 0.5^\circ\text{C}$ for the ONI. During the study period of interest the following episodes were observed: weak La Niña (2000–01), moderate El Niño (2002–03), weak El Niño (2004–05 and 2006–07), moderate La Niña (2007–08) and strong El Niño (2009–10).

The multi-sourced spatio-temporal datasets were collated using the statistical computing software R [32]. Data at the microregion level (i.e. dengue, demographic and cartographic data) and gridded climate data were reconciled by assigning a grid point to each microregion on the basis of the shortest Euclidean distance between microregion centroid and neighbouring grid points.

It should be noted that the nature and availability of both the dengue and the climate data for Brazil, means that the data set is collated at the relatively coarse spatial resolution of the microregion. Therefore, the model formulated in subsequent sections will not be able to capture sub-microregion variations in dengue which are likely influenced by localised meteorological conditions. Rather, the aim in this paper is to identify large scale variations in dengue that could be attributed to seasonal variations in temperature and precipitation which are, in part, driven by the El Niño Southern Oscillation. That said, the ability to provide early warnings of epidemics at the microregion level remains valuable from the point of view of public health decision making and intervention.

4. Model formulation and estimation

Several studies have reported associations between spatial (e.g. [33]) and temporal (e.g. [34, 35]) patterns of dengue and climate. However, these reported associations are not entirely consistent, possibly reflecting the complexity of climatic effects on transmission, and/or the presence of non-climatic confounding factors. Few studies have included non-climatic factors that can affect dengue transmission such as measures of socioeconomic deprivation or levels of urbanisation (e.g. [34, 36, 37]). Many studies do not account for seasonality in the model (e.g. [38, 39]) which can result in misleading inference about dengue-climate relationships. Some models include climate related explanatory variables with multiple possible time lags (e.g. [40]), which can lead to overfitting [11]. Most studies have not tested models on out-of-sample data (e.g. [41]). In addition, appropriate response distributions for count data have not always been employed for modelling dengue cases (e.g. [42]). Otherwise, little allowance has been made for extra-Poisson variation (overdispersion), which is commonly encountered when modelling disease counts and requires attention in model fitting [43].

The model developed in this paper responds to the various points raised above, and refines and extends the model used by the authors [14] in a previous study of dengue risk in Brazil and models used in other studies (e.g. [44] in spatio-temporal analysis of the relationship between annual malaria incidence and selected climate covariates at a district level in Zimbabwe from 1988-1999). The basic modelling framework is a negative binomial (see [45, 46]) generalised linear mixed model (GLMM), where for each spatial location or microregion, $s = (1, \dots, 160)$, and monthly time index, $t = (1, \dots, 108)$, the count of dengue cases, y_{st} , follows a negative binomial distribution with unknown scale parameter, κ , and mean $\mu_{st} = e_{st}\rho_{st}$. Here e_{st} is the expected number of cases, a known offset (based upon the population of microregion s at time t multiplied by the global dengue rate for the whole data set). Then, ρ_{st} is the unknown relative risk for microregion s at time t . A suitable specification for the log relative risk, $\log \rho_{st}$, was then sought via a linear predictor involving climate covariates, non-climate confounding factors, and appropriate spatial and temporal random effects as discussed below.

A series of models of varying complexity, using different subsets of variables, were tested in arriving at a final specification for the form of the linear predictor for $\log \rho_{st}$. These extensive exploratory analyses included the use of formal model selection algorithms based on the 'Akaike Information Criterion' (AIC), supplemented by graphical analyses of fitted values and residuals, examination of model fit with and without climate information, and consideration of the range of other routine model diagnostics. We do not report that model selection process in detail here, but simply comment on some of the issues that were encountered in the process and how we decided to resolve them.

First, considering pure time dependence, we included potential terms in t and powers of t into the linear predictor to allow for any global temporal trend in DIR over the 108 month period covered by the data (years 2001-2009). These were not found to be significant during this period in the presence of the other variables considered. However, DIR does have a marked annual cycle in South East Brazil which peaks in March. To allow for this, an autocorrelated monthly effect was included in the model as a categorical variable for month $t'(t)$, where $t'(\cdot)$ denotes an indicator function which assigns a month marker to the time index t ($t'(t) = 1, \dots, 12$). For convenience, August was set as the reference level ($t'(t) = 1$), since DIR for this month is generally the lowest, so for September, $t'(t) = 2$ and so on. We allowed for the annual cycle in this way because it is a more flexible approach than imposing a parametric sinusoidal form which, whilst it may be mathematically convenient, has little epidemiological justification.

Second, previous studies on DIR in Brazil (see [47] for further details) have shown dengue to be significantly associated with a number of climate factors such as temperature, precipitation and the ONI (an ENSO index), with time lagged values of these variables. For example, Figure 2 shows scatter plots of precipitation/temperature/ONI and DIR for every month (2001-2009) and microregion in South East Brazil. There is a weak positive association between precipitation and dengue incidence (Fig. 2a) and temperature and dengue incidence (Fig. 2b). Further, there is a slight negative relationship between ONI and DIR (relationship consistent at lags ranging from 2 months to 6 months previous, Fig. 2c). We included all of these influences as potential explanatory variables in the linear predictor for $\log \rho_{st}$. Precipitation and temperature covariates lag 1-3 were all found to be statistically significant and these time lags are consistent with previous findings (e.g. [41, 48, 40, 49]). Rather than selecting a particular lag, or including all three lag separately, which could result in over-fitting, these variables were combined into 3-month average precipitation and temperature variables, over the three months preceding the dengue month of interest. This is equivalent to a two month lag when considering the mid point of the three-month average. As our model is intended to be used as an early warning system, this aligns with the fact that temperature and precipitation would in practice be obtained from seasonal climate forecasting systems which are typically issued as seasonal (e.g. December-February average) rather than monthly forecasts. The ONI lagged 2 months and 6 months prior to the dengue month of interest (or 4 months prior to the averaged temperature and precipitation effects) were both favoured by AIC model selection. ONI with lag 6 months prior to the dengue month of interest was selected for inclusion into the model as this provides increased lead time which could be advantageous for a dengue early warning system.

Third, in regard to non-climate factors we included a range of cartographic, demographic and socioeconomic variables

related to the urban environment (see Section 3). Altitude and population density proved to be most important in line with previous findings on DIR in Brazil (see [47] for further details). Altitude was found to have a significant negative association with dengue relative risk while population density was positively associated, as might be intuitively expected.

Fourth, models to predict vector-borne disease have often included autoregressive time series terms (e.g. [50, 51, 40]), based on the idea that current incidence can be partly explained by past values. Clearly, autoregressive terms with one or two month lag offer little, if any, advance warning of an impending epidemic, since, in practice the collation of such data may not be feasible in advance of the time period for which the forecast is valid. However, the number of dengue cases observed several months previously might indicate the presence of increased mosquito populations or the circulation of a new dengue serotype to which the human population is not immune. A lagged dengue relative risk term could then act as a surrogate for unobserved and unmeasured spatio-temporal confounding factors in the model. Accordingly, the variable $z_{st} = \log\left(\frac{y_{st}-3}{e_{st}-3}\right)$, the log ratio of observed to expected dengue cases, i.e. the log standardised morbidity ratio (SMR), lagged by 3 months, was tested in the model. This lag was selected as a compromise between the longest lag plausible to provide predictive skill and the shortest lag possible to allow enough time to provide an early warning of a dengue epidemic. For example, a dengue prediction for March would be based on the dengue risk reported in the previous December. As the inclusion of an autoregressive term causes the first 3 observations in each microregion to be lost, the model was fitted to the data set for the period April 2001- December 2009 (105 months).

Finally, unobserved confounding factors such as population immunity, quality of health care services, and local health interventions are very likely present and important. The inclusion of unstructured random effects in the linear predictor of dengue relative risk can help to account for such unknown or unobserved confounding factors in the disease system. At the same time it is appropriate to include some additional structured random effects into the model to allow for temporal and/or spatial correlation [52]. Such random effects introduce an extra source of variability (a latent effect) into the model which can assist in modelling overdispersion in addition to the single scale parameter in the negative binomial model. Additionally, spatially structured random effects allow for correlated heterogeneity between microregions. A spatial dependency structure can be imposed by assuming a prior distribution for the spatial effects which takes the neighbourhood structure of the area under consideration into account. Prior information which allows for local geographical dependence causes the relative risks in an area to be shrunk towards a local mean, according to the relative risks in neighbouring areas [53]. A typical choice for a spatially structured prior is a conditional intrinsic Gaussian autoregressive model (CAR) (see [54]).

Taking all of the above into account, the final model to emerge from the model selection process comprised a combination of non-climate covariates, lagged climate variables and dengue risk, and spatially and temporally structured and unstructured random effects. The model was formulated as a Bayesian GLMM as follows:

$$\begin{aligned}
 y_{st} | \phi_s, v_s, \omega_{t'(t)} &\sim \text{NegBin}(\mu_{st} = e_{st} \rho_{st}, \kappa), \quad s = 1, \dots, 160, \quad t = 1, \dots, 105 \\
 \log(\mu_{st}) = \log(e_{st}) + \log(\rho_{st}) &= \log(e_{st}) + \alpha + \sum_{j=1}^3 \beta_j x_{jst} + \sum_{j=1}^2 \gamma_j w_{jst} + \delta z_{st} + \phi_s + v_s + \omega_{t'(t)} \\
 \alpha &\sim \text{U}(-\infty, +\infty) \\
 \beta_j &\sim \text{N}(0, 10^6), \quad j = 1, \dots, 3 \\
 \gamma_j &\sim \text{N}(0, 10^6), \quad j = 1, 2 \\
 \delta &\sim \text{N}(0, 10^6) \\
 \phi_s &\sim \text{N}(0, \sigma_\phi^2) \\
 v_s | v_{j \neq s} &\sim \text{CAR}(\sigma_v^2) \\
 \omega_1 = 0, \omega_{t'(t)} | \omega_{t'(t)-1} &\sim \text{N}(\omega_{t'(t)-1}, \sigma_\omega^2), \quad t'(t) = 2, \dots, 12 \\
 \tau_\phi = 1/\sigma_\phi^2 &\sim \text{Ga}(0.5, 0.0005) \\
 \tau_v = 1/\sigma_v^2 &\sim \text{Ga}(0.5, 0.0005) \\
 \tau_\omega = 1/\sigma_\omega^2 &\sim \text{Ga}(0.5, 0.0005) \\
 \kappa &\sim \text{Ga}(0.5, 0.0005).
 \end{aligned}$$

The variables, x_{jst} , ($j = 1, \dots, 3$) represent the selected climate influences: precipitation ($j = 1$) and temperature ($j = 2$) averaged over the previous three months (equivalent to a two month lag), and the ONI four months previous to the local climate variables ($j = 3$). The variables w_{jst} are: altitude ($j = 1$) and population density ($j = 2$). Variable z_{st} is the log dengue SMR three months previously. Spatial random effects are composed of spatially unstructured ϕ_s and structured components v_s . The spatially unstructured random effects, ϕ_s , are assigned independent diffuse Gaussian exchangeable priors and the structured random effects, v_s , are assigned a Gaussian CAR prior. As the formulation of the CAR used here is improper, we follow the usual practice of applying a ‘sum to zero’ constraint to v_s , $s = 1, \dots, 160$, and assigning a uniform flat prior to the model intercept α (see [55] for more details). A first order autoregressive month effect $\omega_{t'(t)}$ is included with month 1 (August) set to zero ($\omega_1 = 0$) and subsequent months following a random walk or first difference prior [56] in which each effect is derived from the immediately preceding effect. Independent diffuse Gaussian priors (mean 0, precision 1×10^{-6}) were taken for the fixed effects β_j ($j = 1, \dots, 3$), γ_j ($j = 1, 2$) and δ . A gamma prior was used for the scale parameter κ . Following [57], weakly informative independent gamma hyperpriors with shape parameter $\zeta = 0.5$ and inverse scale parameter $\eta = 0.0005$ were used for the precisions ($\tau_\phi = 1/\sigma_\phi^2$, $\tau_v = 1/\sigma_v^2$, $\tau_\omega = 1/\sigma_\omega^2$) of the hyperpriors for the spatial and temporal random effects.

The Bayesian model was fitted via MCMC sampling using R in conjunction with WinBUGS software [58] and the R2WinBUGS package [59] (see Supporting Material for model code). Two parallel MCMC chains were generated, each of length 25,000 with a burn-in of 20,000 and thinning of 10 to obtain 1000 samples from the joint posterior distribution. The fixed explanatory variables were standardised to zero mean and unit variance to aid MCMC convergence. MCMC samples from the ‘log-posterior’, i.e. samples from the logarithm of the joint posterior distribution of all model parameters, evaluated at each MCMC iteration can be inspected to give an indication of convergence, since the joint posterior distribution is a global summary of all model parameters. This confirmed satisfactory convergence of the overall model (see Fig 3). To check convergence of the individual parameter estimates, the potential scale reduction \hat{R} (see [60] for details) was calculated (see Table 1, Note: values below 1.1 are considered to be acceptable in most cases, [61]).

Posterior mean parameter estimates are summarised in Table 1. For all parameters (except for population density), the 95% credible interval does not contain zero. This table also includes posterior means for the hyperparameters, relating to the precisions for both spatially structured and unstructured random effects. Figure 4 shows the parameter estimates

and 95% credible intervals for the ‘autocorrelated’ month factor $\omega_{t'(t)}$ in the model. Note that calendar month $t'(t) = 1$ (August) is set as the reference level i.e. its effect is aliased in the model intercept α .

Figure 5a compares observed DIR and fitted posterior mean DIR for all 160 microregions for the 105 month time period (April 2001 - December 2009). Despite the large variability, the superimposed scatter-plot smoother indicates strong overall positive association between observed and model fit DIR. Figure 5b shows the temporal evolution of the fitted posterior mean DIR compared to observed DIR for South East Brazil as a whole. The model is able to correctly detect the inter-annual variability over the time period. The model captures well the magnitude of the DIR in the peak season (February-April (FMA) in 2001, 2006, 2007 and 2008. However, the model underestimated the DIR in 2002 and overestimated in 2004 and 2009, for example.

Figure 6 shows the decomposition of the dengue relative risk across the South East into the climate components ($\exp(\beta_1 x_{1st} + \beta_2 x_{2st} + \beta_3 x_{3t})$, see Fig 6a) and the dengue risk three months previous ($\exp(\delta z_{st})$, see Fig 6b). This allows us to identify the relative contribution of the spatio-temporal covariates in the model and their spatio-inter-annual variability for the peak dengue season February - April (FMA) in 2005 (a non-epidemic year, row 1) and 2008 (an epidemic year, row 2). The spatial distribution of the model fit DIR (including all data, parameter estimates and random effects) and observed DIR are shown in Figure 6c and d respectively.

5. Predictions for dengue epidemics

In order to quantify the predictive benefit of the model and to ensure the efficacy of the modelling framework to public health decision makers, it is important to assess how well the developed model can predict future and also geographically specific dengue epidemics. For that purpose, the model was fitted to data from April 2001 - December 2007 and posterior predictive distributions [62] were then derived for dengue counts for the out-of-sample data from January 2008 - December 2009.

The current monitoring system in Brazil relies on observing an increase in early cases around 3 months prior to the onset of the peak dengue season. To test if the spatio-temporal model developed in the previous section performs better than current practice, that model is compared to a simple model which essentially reflects current dengue surveillance in Brazil i.e.:

$$y_{st} \sim \text{NegBin}(\mu_{st}, \kappa)$$

$$\log \mu_{st} = \log e_{st} + \alpha + \delta z_{st},$$

with the expected number of cases e_{st} as the model offset and the variable $z_{st} = \log\left(\frac{y_{st-3}}{e_{st-3}}\right)$ being the log of the ratio of observed to expected cases lagged by 3 months, as previously defined. We will refer to this as the current surveillance model (CSM). Note that this is a sub-model of the GLMM specified the previous section.

The out-of-sample posterior predictions for January 2008 - December 2009 from the GLMM and CSM were compared with observations for each of the 160 microregions in South East Brazil. Figure 7 shows the spatial distribution of observed and predicted DIR using both models for the FMA season 2008–2009. Although the GLMM has a tendency to over predict DIR in certain areas, the model is better able to capture instances of very high DIR across the South East region. In general the CSM predicts low to medium DIR for most of the region even when high DIR is observed. Despite some false alarms (i.e. high DIR predicted when low DIR observed), there are more instances where the GLMM successfully detected high DIR compared to the CSM (e.g. east coast 2008, Fig. 7.1a, b and c). Overall, the CSM fails to capture the observed DIR behaviour across the region.

In general, dengue warnings are most useful at the microregion level, to allow local governments to make decisions on resource allocation. With this in mind, it is useful to select some key large microregions in SE Brazil for further inspection.

Belo Horizonte (population of 4,932,777) and Rio de Janeiro (population of 11,554,872) were chosen as they contain the capital cities of the states of Minas Gerais and Rio de Janeiro, respectively. As São Paulo experienced comparatively low DIR during the out-of-sample period, another large microregion in that state was selected: São Jose dos Campos (population of 1,381,846). In Figure 8, observed DIR, the mean of the posterior predictive distribution and 95% credible intervals, calculated using the 2.5% and 97.5% quantiles of the posterior predictive distribution, are presented for these three microregions; Belo Horizonte, Rio de Janeiro and São Jose dos Campos. In general, the GLMM better captured the temporal behaviour of DIR than the CSM. The GLMM was also able to predict that the dengue season for Belo Horizonte was equally high in 2009 as in 2008 (see Fig. 8.1a). For microregions Rio de Janeiro and São Jose dos Campos the GLMM over-predicted the 2009 season but again better captured the temporal behaviour in dengue than the CSM (see Fig. 8.1b, 8.2b, 8.1c and 8.2c).

The GLMM and CSM can be used to predict the probability of dengue exceeding a pre-defined epidemic threshold in each microregion. As the posterior predictive distribution can be obtained for each microregion (rather than a point estimate), the probability of exceeding an epidemic threshold can be calculated. The decision to trigger an alert can be based on the probability of exceeding the threshold being greater than a specified alert level, (e.g. a probability of exceedance greater than 50%). As an example, the event of dengue incidence exceeding 300 cases per 100,000 inhabitants ($DIR > 300$; high incidence threshold defined by the National Dengue Control Programme in Brazil) is considered. In March 2008, a serious epidemic occurred across parts of Brazil, that originated in Rio de Janeiro. As a further illustration of the weakness of the CSM as a prediction tool, it is interesting to note that the posterior predictive probability of $DIR > 300$, obtained from the CSM is less than 50% for all microregions during the major epidemic in FMA, 2008. On the other hand, the GLMM highlights 44 microregions as having more than a 50% chance of $DIR > 300$ (note that 54 microregions experienced $DIR > 300$). For example, in Rio de Janeiro, the CSM gave a probability of exceeding 300 cases per 100,000 inhabitants of 0.37 whereas for the GLMM, the probability of exceedance was 0.75 (see Fig. 9).

Although the GLMM produces a considerable number of false alarms compared to the CSM, it is capable of detecting elevated levels of DIR which is important for an early warning system to help direct the allocation of resources to cope with area-specific dengue epidemics. We conclude that the GLMM is an improvement to current practice and that the inclusion of climate information and observed and unobserved confounding factors improves the performance of the model. The remainder of the paper focuses on the usefulness of the developed model to public health decision makers.

6. Probability decision thresholds

One way to evaluate probabilistic forecasts of any event is to consider the set of deterministic binary forecasts obtained by choosing a range of probability decision thresholds [63]. The ability of the GLMM to predict dengue epidemics across South East Brazil during the 2008 epidemic (FMA season) can be assessed by comparing observed DIR for the 3-month season FMA 2008 with model predictions with varying probability decision thresholds. During this season, 54 of the 160 microregions in South East Brazil experienced an 'epidemic' ($DIR > 300$). A 2×2 contingency table then provides information on the overall predictive skill of the warning system given a specific threshold. For example, given a probability decision threshold of 60%, the proportion correct (PC), defined as the proportion of the 160 microregions for which the prediction correctly anticipated the subsequent epidemic or non-epidemic, $(a + d)/(a + b + c + d)$, was 76%. The hit rate (HR); the proportion of epidemics that were correctly predicted $(a/(a + c))$, also known as sensitivity), was 57%. Conversely, the false alarm rate (FAR); the proportion of epidemics that were predicted but did not occur $(b/(b + d))$, also known as 1-specificity), was 12% (see Table 2). When the probability decision threshold was lowered to 40%, PC = 74%, HR = 91% and FAR = 34%. By lowering the probability decision threshold, the hit rate for the region increases but so does the false alarm rate.

Clearly, a single set of binary forecasts does not provide a satisfactory basis for assessment of the quality of the

forecasting system [64]. This is because it shows the performance of the system at only a single probability decision threshold. A complete description of predictive skill requires verification over the full range of possible thresholds. An analysis tool that accomplishes this is the Relative (or Receiver) Operating Characteristic (ROC) graph of the hit rate against the false alarm rate (or sensitivity against 1-specificity) for different decision thresholds. As the probability decision threshold varies from high to low (moving from left to right) HR and FAR vary together to trace out the ROC curve. Perfect discrimination is represented by the point (0,1) where HR= 100% and FAR= 0%. The diagonal HR=FAR represents zero skill, i.e. the forecasting system performs as well as random guessing. The area under the modelled ROC curve, abbreviated AUC [65], is a widely used ROC-based measure of skill. AUC characterises the quality of a forecast system by describing the system's ability to anticipate correctly the occurrence or non-occurrence of pre-defined events [66]. The possible range of AUC is [0, 1]. Zero skill is indicated by AUC=0.5, i.e. area under the diagonal HR=FAR. For perfect skill, AUC=1. To test the null hypothesis that the area under the ROC curve is 0.5, i.e. the forecast has no skill, a p-value can be calculated using a Mann-Whitney *U*-test (see [66]). Figure 10 shows the ROC curve for dengue epidemics during the FMA season 2008 using the GLMM for the 160 microregions in South East Brazil, with AUC=0.86 (p-value $\ll 0.05$). This indicates that the forecasting system is significantly more skillful than randomly guessing. By lowering the probability decision threshold, the hit rate increases but so does the false alarm rate. Optimal probability decision thresholds are sometimes determined as the point where the ROC curve intersects the negative 45° line (where sensitivity=specificity or HR=1-FAR) or the point where the distance from the HR=FAR line is greatest [67]. In practice, the choice of epidemic threshold and probability decision thresholds should be decided based on expert opinion and available resources.

7. Presenting dengue forecasts to decision makers

If a 'forecasting system' is capable of producing probabilistic forecasts over a geographical area, these forecasts can be displayed graphically in the form of a map. This may be useful for targeting resource allocation to areas most at risk. To communicate information contained in a probabilistic forecast, we adopt a new method for visualising ternary probabilistic forecasts, i.e. forecasts that assign probabilities to a set of three mutually exclusive and complete outcomes (e.g. low, medium and high risk). This method is described in more detail in [68]. The idea is to consider a ternary forecast as a point in a triangle of barycentric coordinates. This allows a unique colour to be assigned to each forecast from a continuum of colours defined on the triangle. Colour saturation increases with information gain relative to the reference forecast. This provides additional information to decision makers compared to conventional methods used in seasonal climate forecasting, where one colour is used to represent one forecast category on a forecast map (e.g. red='dry').

As posterior predictive distributions for dengue incidence rates can be derived from the model for each microregion and month, the probability of dengue risk falling into pre-defined categories can be calculated. The Brazilian Ministry of Health are interested in areas where $DIR \leq 100$; indicating low risk, $100 < DIR \leq 300$; indicating medium risk and $DIR > 300$; indicating high risk. Using this new method, maps can be produced in which the forecast at each geographical location is expressed as a colour determined by a combination of three probabilities.

Given the pre-defined categories boundaries, the model can produce probabilistic forecasts, p_1 (probability of low risk category), p_2 (probability of medium risk category), p_3 (probability of high risk category), that dengue incidence rates will be in each category at the forecast time. The probability forecast can be regarded as $\mathbf{p} = (p_1, p_2, p_3)$ with the constraints $p_1 + p_2 + p_3 = 1$ and $0 \leq p_i \leq 1, \forall i$. The particular forecast $\mathbf{q} = (q_1, q_2, q_3)$ corresponds to the case where the forecaster's state of knowledge is 'no better' than the historical observed distribution. For example, if the forecaster had no knowledge other than the observational record, the same forecast \mathbf{q} could be issued each year. Here, \mathbf{q} will be referred to as the reference forecast; a benchmark distribution with which all other forecasts can be compared.

According to the observed distribution for the FMA season 2001-2007, 65% of the values fell below $DIR = 100$, 12% fell between $DIR = 100$ and $DIR = 300$, and 23% fell above $DIR = 300$ (see density plot in Fig 11). As the categories

apply to a dengue rate (cases per 100,000 inhabitants), rather than absolute counts, the category boundaries are the same for each spatial location. Therefore, the reference forecast \mathbf{q} becomes $\mathbf{q} = (0.65, 0.12, 0.23)$. When representing probabilistic forecasts using colour, determined from a point in a triangle of barycentric coordinates (see [68]), the reference forecast (\times) can be located at a point which satisfies these 3 probabilities (see triangle in Fig. 11). Using these category boundaries, blue is assigned to the low risk category, yellow to the medium risk category and red to the high risk category.

Figure 12a presents a probabilistic forecast map of DIR for FMA season 2008 using the GLMM. The observed DIR category for each microregion is shown for comparison (Fig. 12b). For the FMA season 2008, the GLMM would have correctly forecast high DIR for Rio de Janeiro and microregions along the east coast and in the west of the region (darker shades of red) and would have correctly forecast low DIR in the South (darker shades of blue). The map also shows areas where the model was uncertain as to which dengue category might be observed (pale shades). Communicating information contained within a probabilistic forecast presents a challenge. It is hoped that this visualisation method may facilitate the interpretation of the probabilistic forecasts of dengue incidence rates from the model for public health decision makers.

8. Discussion

This paper highlights the potential for incorporating climate information into a spatio-temporal dengue epidemic early warning system for South East Brazil. The use of climate variables in conjunction with other factors in a GLMM improves on current practice for dengue surveillance and control in Brazil. This work builds on several previous climate and health studies by moving away from simple models at the country level, involving only temporal variations in climate and disease, to a more sophisticated spatio-temporal model providing probabilistic predictions that can aid decision making and target resource allocation. This model allows for extra-Poisson variation via a negative binomial formulation, for the annual cycle via temporally correlated month effects and for unobserved confounding factors and spatial correlation through spatially unstructured and spatially structured random effects.

The GLMM was fitted using a Bayesian estimation framework allowing posterior predictive distributions for disease risk to be derived at each spatial location for a given month or season. This allowed probabilistic forecasts to be issued. An evaluation of the forecast skill of dengue epidemic warnings using out-of-sample data was conducted. The model was compared to a simple conceptual model of current practice, based on dengue cases three months previously. It was found that the developed model including climate, past dengue risk and observed and unobserved confounding factors, enhanced dengue predictions compared to model based on past dengue risk alone.

A major obstacle to developing a climate-driven dengue model is the lack of high quality climate and disease data over long time periods. A further disadvantage is that the available dengue data is not broken down by virus type. Serological information could be useful to indicate the periodicity of circulating serotypes (DENV-1, DENV-2, DENV-3, DENV-4) which influence population immunity and hence the occurrence of epidemics. Further, as temperature and precipitation influence the abundance and transmission potential of *Aedes Aegypti*, it would be advantageous to include entomological data in the analysis. However, this information was unobtainable.

Another potentially important component missing from the model is the seasonal movement of human hosts around Brazil. The proximity matrix used to formulate the CAR prior for the spatially structured random effects in the GLMM, assumes a simple local structure where each microregion is dependent only on its neighbours. However, certain areas may be more closely related, in terms of dengue transmission, to remote areas connected by air or road transport links, rather than neighbouring microregions. IBGE have released a new study entitled 'Areas of Influence of Cities' based on research into the Brazilian urban network. A hierarchy of urban centres is defined based on the flow of good and services, including air and road travel. A proximity matrix based on this hierarchical matrix might improve the correlation structure within the model.

The spatio-temporal hierarchical model is intended to become part of a newly established climate and health

observatory in Brazil (<http://www.inpe.br/noticias/arquivos/pdf/observatorium.pdf>). However, before implementing such an operational system, several technical issues need to be considered. In practice, observed climate could be replaced by climate forecasts which might extend the lead time beyond that offered by using lagged observations. By replacing observed with forecast climate variables in the model, a dengue prediction could be made several months ahead of the dengue season of interest. For example, to predict dengue incidence for March 2012, the model could be run in November 2011 using the observed ONI for August–October 2011 (6 month lag), and precipitation and temperature forecasts for December–February 2011–2012 issued in November 2011 (see Fig 13). The dengue risk at the time of forecast (e.g. November) could be used as a best guess for dengue risk three months previous to the month of interest (e.g. March). This would provide a four month lead time, which could allow time for the allocation of resources to interventions such as preparing health care services for increased numbers of dengue patients and educating populations to eliminate mosquito breeding sites. However, the efficacy of a climate-based epidemic early warning system will depend on the skill of the climate forecasting system. One such system that is operational in Brazil and shows some skill in South East Brazil is the EUROBRISA initiative [69] which is a multi-model combined and calibrated system that produces one-month lead precipitation forecasts for the following three-month season.

Probability alert thresholds should be carefully designed to minimise false alarms and false negatives (i.e. failing to predict that an epidemic will occur) and should correspond with the epidemic response capabilities of the region where the model might be implemented. An important issue is the consideration of future interventions in the model framework. If the Brazilian health services respond to an early warning of a dengue epidemic and take measures to reduce the impact, an apparent false alarm may in fact be the result of a successful intervention.

Acknowledgements

GPCP precipitation and NCEP/NCAR reanalysis temperature data was provided by the NOAA/OAR/ESRL PSD, Boulder, Colorado, USA, from their Web site at <http://www.esrl.noaa.gov/psd/>. RL would like to thank Evangelina Xavier Gouveia de Oliveira (IBGE) for kindly providing socioeconomic/geographical data, Adrian Tompkins (ICTP) for insights into dynamical modelling and Caio Coelho (CPTEC) for useful discussions about the application of seasonal climate forecasts in Brazil.

References

1. Gage K, Burkot T, Eisen R, Hayes E. Climate and vectorborne diseases. *American Journal of Preventive Medicine* 2008; **35**(5):436–450.
2. Kovats RS, Bouma MJ, Hajat S, Worrall E, Haines A. El Niño and health. *Lancet* 2003; **362**(9394):1481–1489.
3. Kelly-Hope L, Thomson MC. Climate and infectious diseases. In: *Seasonal Forecasts, Climatic Change and Human Health* 2008; :31–70.
4. Thomson MC, Doblas-Reyes FJ, Mason SJ, Hagedorn R, Connor SJ, Phindela T, Morse AP, Palmer TN. Malaria early warnings based on seasonal climate forecasts from multi-model ensembles. *Nature* 2006; **439**(7076):576–579.
5. Cox J, Abeku T. Early warning systems for malaria in Africa: from blueprint to practice. *Trends in Parasitology* 2007; **23**(6):243–246.
6. Ebi K. Malaria Early Warning Systems. In: *Biometeorology for Adaptation to Climate Variability and Change* 2009; :49–74.
7. Githeko A, Ndegwa W. Predicting malaria epidemics in the Kenyan highlands using climate data: a tool for decision makers. *Global Change & Human Health* 2001; **2**(1):54–63.
8. Hoshen M, Morse A. A weather-driven model of malaria transmission. *Malaria Journal* 2004; **3**(32):14pp.
9. Worrall E, Connor SJ, Thomson MC. A model to simulate the impact of timing, coverage and transmission intensity on the effectiveness of indoor residual spraying (IRS) for malaria control. *Tropical Medicine & International Health* 2007; **12**(1):75–88.
10. Jones AE, Morse AP. Application and validation of a seasonal ensemble prediction system using a dynamic malaria model. *Journal of Climate* 2010; **23**(15):4202–4215.
11. Lafferty KD. The ecology of climate change and infectious diseases. *Ecology* 2009; **90**(4):888–900.
12. Teixeira M, Costa M, Barreto F, Barreto M. Dengue: twenty-five years since reemergence in Brazil. *Cadernos de Saúde Pública* 2009; **25**:7–18.

13. Gubler D. How effectively is epidemiological surveillance used for dengue programme planning and epidemic response? *Dengue Bulletin* 2002; **26**:96–106.
14. Lowe R, Bailey TC, Stephenson DB, Graham RJ, Coelho CAS, Carvalho MS, Barcellos C. Spatio-temporal modelling of climate-sensitive disease risk: Towards an early warning system for dengue in Brazil. *Computers & Geosciences* 2011; **37**:371–381.
15. Gubler DJ. Epidemic dengue/dengue hemorrhagic fever as a public health, social and economic problem in the 21st century. *Trends in Microbiology* 2002; **10**(2):100–103.
16. Guzman MG, Kouri G. Dengue and dengue hemorrhagic fever in the Americas: lessons and challenges. *Journal of Clinical Virology* 2003; **27**(1):1–13.
17. Rigau-Pérez J, Clark G, Gubler D, Reiter P, Sanders E, Vance Vorndam A. Dengue and dengue haemorrhagic fever. *The Lancet* 1998; **352**(9132):971–977.
18. Reiter P. Climate change and mosquito-borne disease. *Environmental Health Perspectives* 2001; **109**(Suppl 1):141–161.
19. Chambers T, Hahn C, Galler R, Rice C. Flavivirus genome organization, expression, and replication. *Annual Reviews in Microbiology* 1990; **44**(1):649–688.
20. Halstead SB. The Alexander D. Langmuir Lecture. The pathogenesis of dengue. Molecular epidemiology in infectious disease. *American Journal of Epidemiology* 1981; **114**(5):632–648.
21. McMichael AJ, Haines A, Slooff S R Kovats. Climate change and human health: an assessment prepared by a Task Group on behalf of the World Health Organization, the World Meteorological Organization and the United Nations Environment Programme. *World Health Organization, Geneva* 1996; :297pp.
22. Gubler DJ. Dengue and Dengue Hemorrhagic Fever. *Clinical Microbiology Reviews* 1998; **11**(3):480–496.
23. Gubler D, Meltzer M. Impact of dengue/dengue hemorrhagic fever on the developing world. *Advances in Virus Research* 1999; **53**:35–70.
24. Favier C, Degallier N, Dubois MA. Dengue epidemic modelling: stakes and pitfalls. *Asia Pacific Biotech News* 2005; **9**(22):1191–1194.
25. Halstead S, Deen J. The future of dengue vaccines. *Lancet* 2002; **360**(9341):1243–1245.
26. Webster D, Farrar J, Rowland-Jones S. Progress towards a dengue vaccine. *The Lancet Infectious Diseases* 2009; **9**(11):678–687.
27. Siqueira J, Martelli C, Coelho G, Simplício A, Hatch D. Dengue and dengue hemorrhagic fever, Brazil, 1981–2002. *Emerging Infectious Diseases* 2005; **11**(1):48–53.
28. Nogueira RMR, da Araújo JMG, Schatzmayr HG. Aspects of dengue virus infections in Brazil 1986–2007. *Virus Reviews and Research* 2007; **12**:1–17.
29. Adler RF, Susskind J, Huffman GJ, Bolvin D, Nelkin E, Chang A, Ferraro R, Gruber A, Xie PP, Janowiak J, *et al.*. The version-2 global precipitation climatology project (GPCP) monthly precipitation analysis (1979–present). *Journal of Hydrometeorology* 2003; **4**(6):1147–1167.
30. Kalnay E, Kanamitsu M, Kistler R, Collins W, Deaven D, Gandin L, Iredell M, Saha S, White G, Woollen J, *et al.*. The NCAR/NCEP 40-year reanalysis project. *Bulletin of the American Meteorological Society* 1996; **77**(3):437–471.
31. Philander S. *El Niño, La Niña, and the Southern Oscillation*. Academic Press, USA, 293pp, 1990.
32. R Development Core Team. *R: A Language and Environment for Statistical Computing*. R Foundation for Statistical Computing, Vienna, Austria 2009. URL <http://www.R-project.org>, ISBN 3-900051-07-0.
33. Hales S, de Wet N, Maindonald J, Woodward A. Potential effect of population and climate changes on global distribution of dengue fever: an empirical model. *The Lancet* 2002; **360**(9336):830–834.
34. Hales S, Weinstein P, Souares Y, Woodward A. El Niño and the dynamics of vectorborne disease transmission. *Environmental Health Perspectives* 1999; **107**(2):99–102.
35. Gagnon AS, Bush ABG, Smoyer-Tomic KE. Dengue epidemics and the El Niño Southern Oscillation. *Climate Research* 2001; **19**(1):35–43.
36. Chakravarti A, Kumaria R. Eco-epidemiological analysis of dengue infection during an outbreak of dengue fever, India. *Virology Journal* 2005; **2**(1):32–38.
37. Câmara FP, Gomes AF, Santos GT, Câmara DC. Climate and dengue epidemics in State of Rio de Janeiro. *Revista de Sociedade Brasileira de Medicina Tropical* 2009; **42**(2):137–140.
38. Nakhapakorn K, Tripathi NK. An information value based analysis of physical and climatic factors affecting dengue fever and dengue haemorrhagic fever incidence. *International Journal of Health Geographics* 2005; **4**(13):13pp.
39. Promprou S, Jaroensutasinee M, Jaroensutasinee K. Climatic factors affecting dengue haemorrhagic fever incidence in Southern Thailand. *Dengue Bulletin* 2005; **29**:41–48.
40. Tipayamongkolgul M, Fang C, Klinchan S, Liu C, King C. Effects of the El Niño-Southern Oscillation on dengue epidemics in Thailand, 1996–2005. *BMC Public Health* 2009; **9**(422):15pp.
41. Schreiber KV. An investigation of relationships between climate and dengue using a water budgeting technique. *International Journal of Biometeorology* 2001; **45**:81–89.
42. Arcari P, Tapper N, Pfueller S. Regional variability in relationships between climate and dengue/DHF in Indonesia. *Singapore Journal of Tropical Geography* 2007; **28**(3):251–272.
43. Crawley MJ. *Statistical Computing: An Introduction to Data Analysis using S-Plus*. John Wiley & Sons Ltd, UK, 761pp, 2002.
44. Mabaso M, Vounatsou P, Midzi S, Da Silva J, Smith T. Spatio-temporal analysis of the role of climate in inter-annual variation of malaria incidence in Zimbabwe. *International Journal of Health Geographics* 2006; **5**(20):9pp.

45. McCullagh P, Nelder J. *Generalized Linear Models, Second Edition*. Chapman Hall, London, UK, 536pp, 1989.
46. Venables WN, Ripley BD. *Modern Applied Statistics With S*. Springer, New York, USA, 495pp, 2002.
47. Lowe R. Spatio-temporal modelling of climate-sensitive disease risk: towards an early warning system for dengue in Brazil. PhD Thesis, University of Exeter 2010.
48. Wu P, Guo H, Lung S, Lin C, Su H. Weather as an effective predictor for occurrence of dengue fever in Taiwan. *Acta Tropica* 2007; **103**(1):50–57.
49. Johansson MA, Dominici F, Glass G. Local and Global Effects of Climate on Dengue Transmission in Puerto Rico. *PLoS Neglected Tropical Diseases* 2009; **3**(2):e382.
50. Zhou G, Minakawa N, Githeko A, Yan G. Association between climate variability and malaria epidemics in the East African highlands. *Proceedings of the National Academy of Sciences of the United States of America* 2004; **101**(8):2375–2380.
51. Gomez-Elipe A, Otero A, Van Herp M, Aguirre-Jaime A. Forecasting malaria incidence based on monthly case reports and environmental factors in Karuzi, Burundi, 1997–2003. *Malaria Journal* 2007; **6**(129):10pp.
52. Lawson A. *Bayesian Disease Mapping: Hierarchical Modeling in Spatial Epidemiology*. Chapman & Hall/CRC, Boca Raton, Florida, USA, 344pp, 2008.
53. Mollie A. Bayesian mapping of disease. *In: Markov Chain Monte Carlo in Practice* 1996; :359–379.
54. Besag J, Green P, Higdon D, Mengersen K. Bayesian computation and stochastic systems. *Statistical Science* 1995; **10**(1):3–41.
55. Best N, Arnold R, Thomas A, Waller L, Conlon E. Bayesian models for spatially correlated disease and exposure data. *Bayesian Statistics* 1999; **6**:131–156.
56. Gilks WR, Richardson S, Spiegelhalter DJ. *Markov Chain Monte Carlo in Practice*. Chapman & Hall/CRC, Boca Raton, Florida, USA, 486pp, 1996.
57. Wakefield JC, Best NG, Waller L. Bayesian approaches to disease mapping. *In: Spatial Epidemiology: Methods and Applications* 2000; :104–127.
58. Lunn D, Thomas A, Best N, Spiegelhalter D. WinBUGS—a Bayesian modelling framework: concepts, structure, and extensibility. *Statistics and Computing* 2000; **10**(4):325–337.
59. Sturtz S, Ligges U, Gelman A. R2WinBUGS: a package for running WinBUGS from R. *Journal of Statistical Software* 2005; **12**(3):1–16.
60. Gelman A, Rubin DB. Inference from iterative simulation using multiple sequences. *Statistical Science* 1992; **7**(4):457–472.
61. Gelman A, Carlin J, Stern H, Rubin D. *Bayesian Data Analysis, Second Edition*. Chapman & Hall/CRC, Boca Raton, Florida, USA, 668pp, 2004.
62. Gelman A, Meng X, Stern H. Posterior predictive assessment of model fitness via realized discrepancies. *Statistica Sinica* 1996; **6**:733–759.
63. Mason I. On reducing probability forecasts to yes/no forecasts. *Monthly Weather Review* 1979; **107**(2):207–211.
64. Mason I. Binary Events. *In: Forecast Verification: A Practitioners Guide in Atmospheric Science*, 37–76 2003.
65. Fawcett T. An introduction to ROC analysis. *Pattern Recognition Letters* 2006; **27**(8):861–874.
66. Mason SJ, Graham NE. Areas beneath the relative operating characteristics (roc) and relative operating levels (rol) curves: Statistical significance and interpretation. *Quarterly Journal of the Royal Meteorological Society* 2002; **128**(584):2145–2166.
67. Pepe MS. *The Statistical Evaluation of Medical Tests for Classification and Prediction*. Oxford University Press, USA, 302pp, 2004.
68. Jupp T, Lowe R, Stephenson DB, Coelho CAS. On the visualisation, verification and recalibration of ternary probabilistic forecasts. *Philosophical Transactions of the Royal Society A [in press]* 2011; .
69. Coelho CAS, Stephenson DB, Balmaseda M, Doblas-Reyes FJ, van Oldenborgh GJ. Toward an integrated seasonal forecasting system for South America. *Journal of Climate* 2006; **19**(15):3704–3721.

9. Tables and Figures

Table 1. Parameter estimates and convergence diagnostic \hat{R} for covariates and hyperparameters associated with the spatial and temporal random effects. CI is the credible interval obtained from the 2.5% and 97.5% quantiles of the distribution.

	mean	standard deviation	95% CI	\hat{R}
Precipitation	0.317	0.035	[0.246, 0.387]	1.029
Temperature	0.503	0.037	[0.435, 0.580]	1.071
Oceanic Niño Index	-0.412	0.022	[-0.456, -0.368]	1.000
Altitude	-0.964	0.080	[-1.119, -0.812]	1.023
Population density	0.065	0.055	[-0.041, 0.174]	1.056
Lagged dengue risk	0.214	0.004	[0.205, 0.222]	1.003
Spatially unstructured hyperparameter	11485.052	1276.669	[102.615, 4697.996]	1.091
Spatially structured hyperparameter	0.508	0.066	[0.390, 0.652]	1.001
Temporally structured hyperparameter	2.74	1.159	[0.922, 5.378]	1.000
Scale parameter	0.470	0.006	[0.458, 0.483]	1.001

Table 2. Summary of contingency table results for observed dengue incidence exceeding epidemic threshold of 300 cases per 100,000 inhabitants at varying probability decision thresholds (60%, 50%, 40%) for the 160 microregions FMA 2008 using GLMM. *a* is the number of events correctly forecast to occur (hits); *b* is the number of events incorrectly forecast to occur, (false alarms); *c* is the number events incorrectly forecast not to occur, (misses); and *d* is the number of event correctly forecast not to occur (correct rejections). PC is proportion correct, HR is hit rate and FAR is false alarm rate.

Threshold	a	b	c	d	PC	HR	FAR
60%	31	13	23	93	76%	57%	12%
50%	44	27	10	79	77%	81%	25%
40%	49	36	5	70	74%	91%	34%

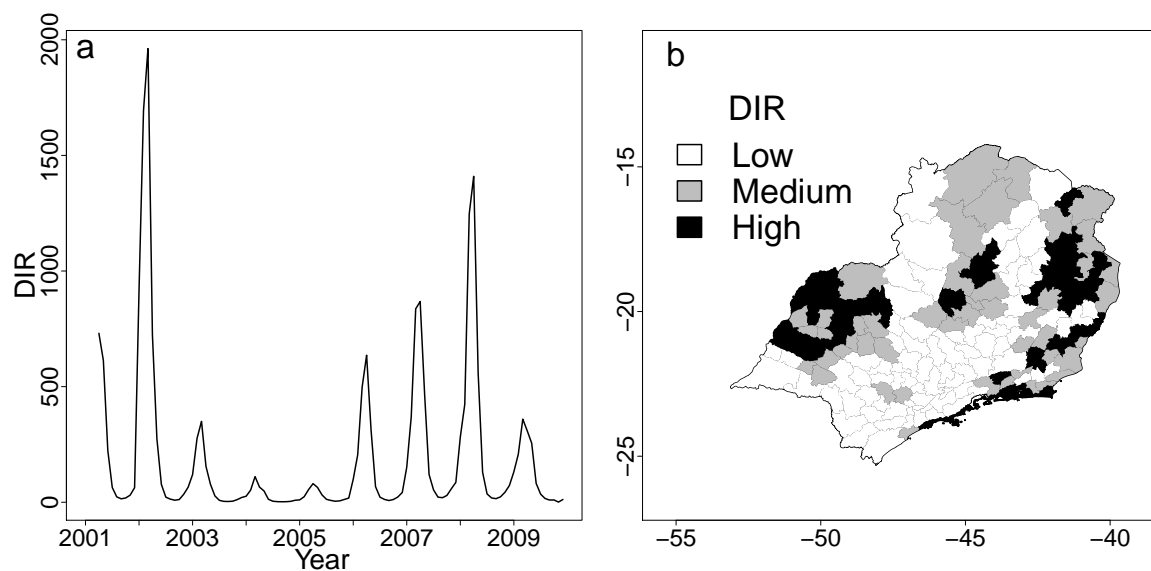


Figure 1. (a) Dengue incidence rate (DIR) for South East Brazil January 2001 - December 2009. (b) Map of low (less than 100), medium (between 100 and 300) and high (greater than 300) dengue incidence in each microregion over 2001-2009.

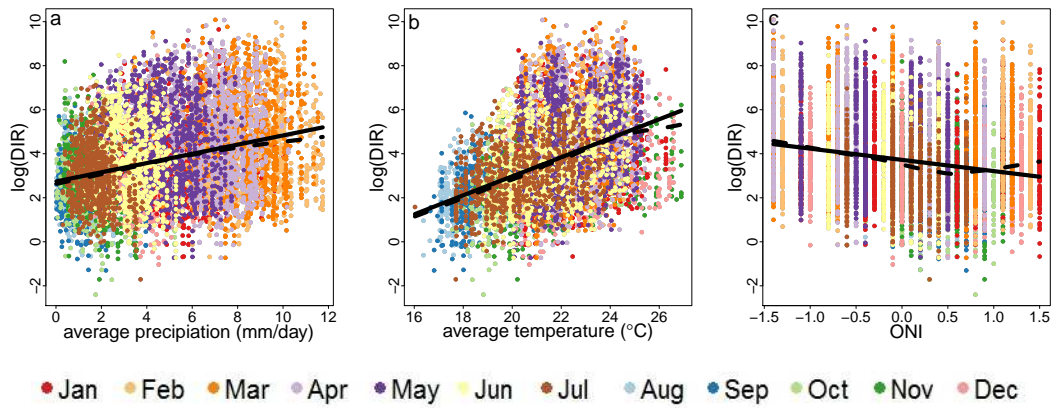


Figure 2. Scatter plot between $\log(\text{DIR})$ and (a) precipitation, (b) temperature (averaged over 3 months previous to dengue month) and (c) ONI (lagged 4 months previous to local climate variables). Solid curve - linear model fit, dashed curve - local polynomial regression fit. Note points stratified by calendar month for DIR.

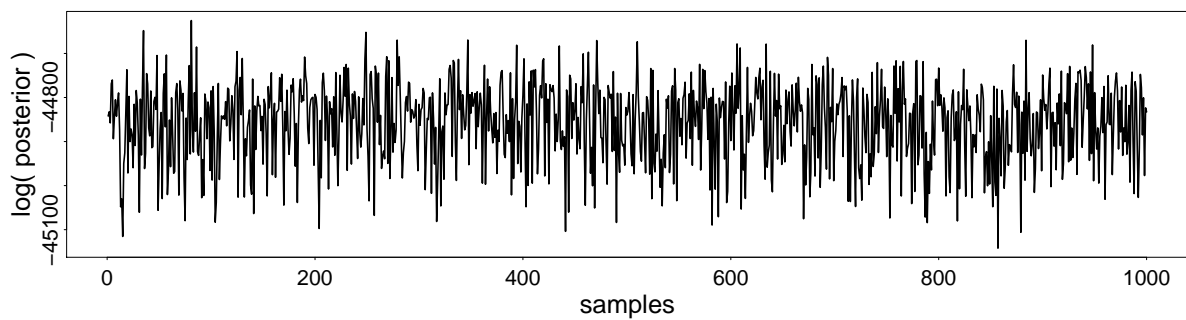


Figure 3. Trace plot of log posterior distribution for 1000 samples from the model.

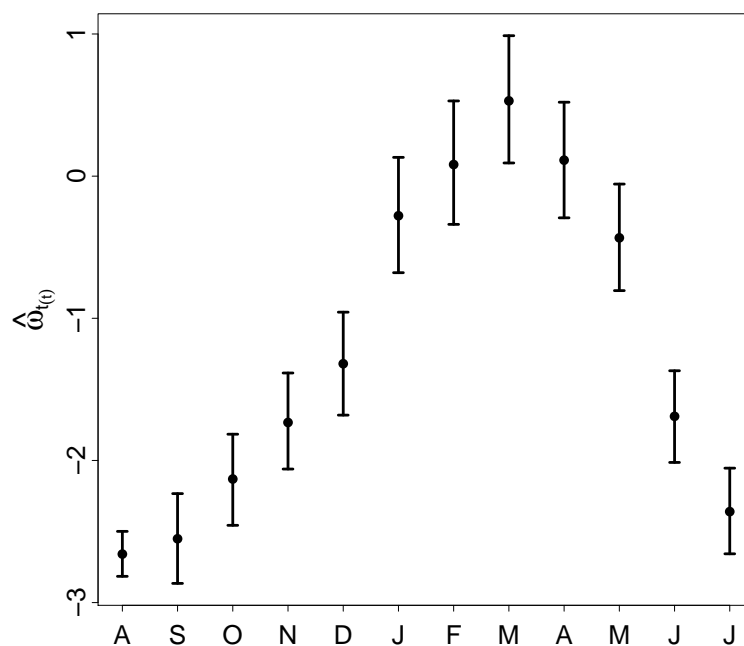


Figure 4. Parameter estimates (circle) and 95% credible intervals (bars) for autocorrelated month effect $\hat{\omega}_{t'(t)}$.

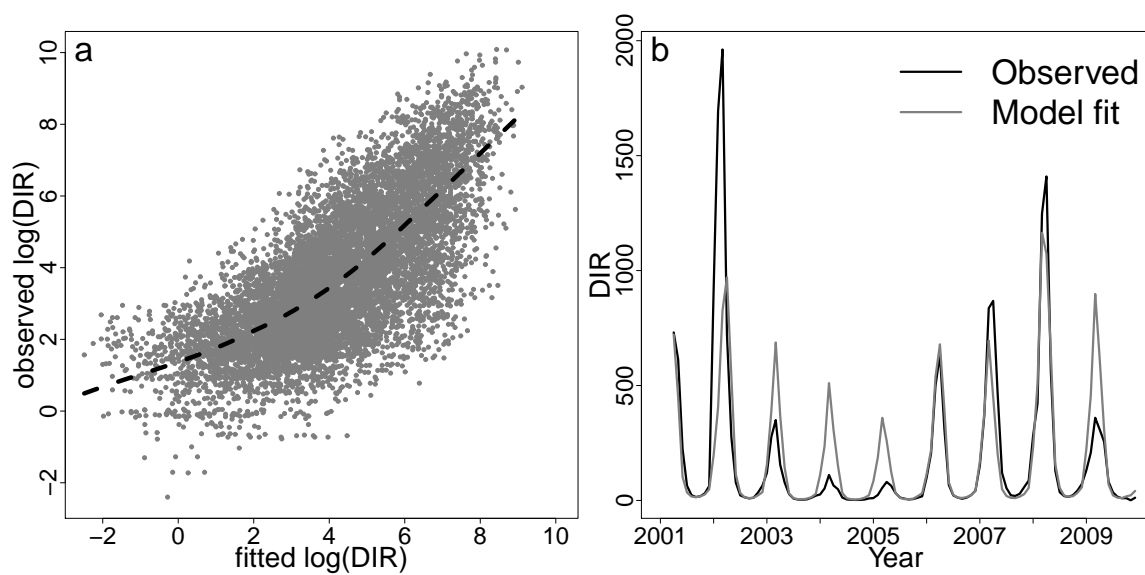


Figure 5. Observed and model fit DIR at the linear predictor level for all months (105) and microregions (160). Dashed curve - local polynomial regression fit. (b) Total observed (black line) and model fit (grey line) DIR from April 2001 - December 2009.

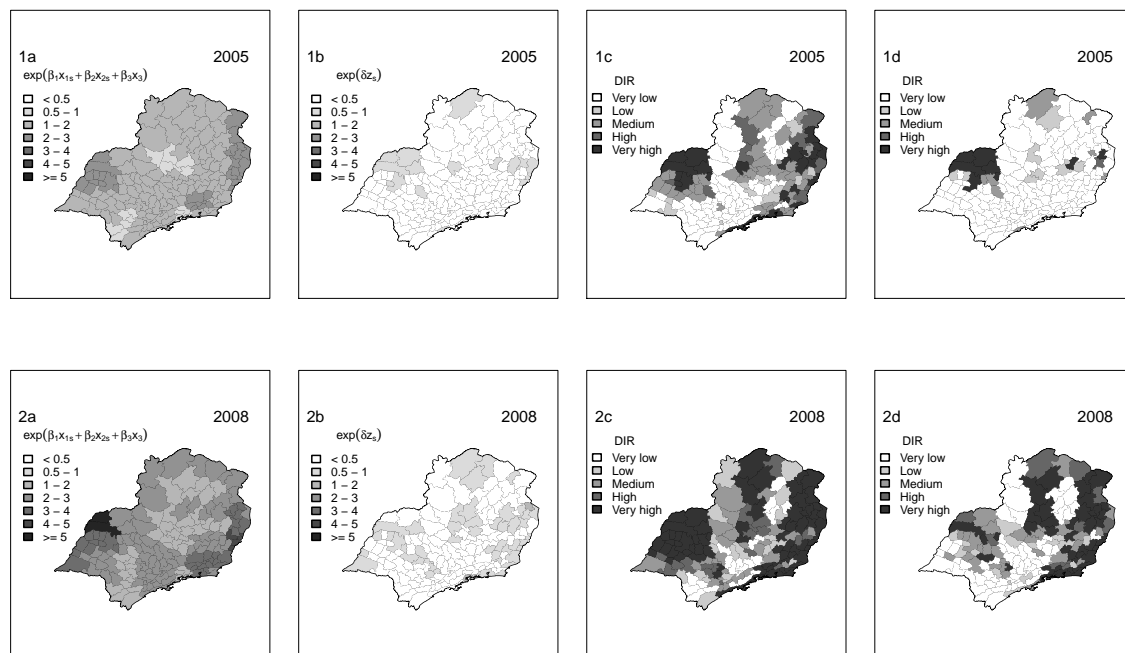


Figure 6. Multiplicative decomposition of the dengue relative risk map in South East Brazil into (a) the climate component explained by precipitation, temperature and ONI and (b) dengue relative risk 3 month previous. (c) Model fit and (d) observed DIR in South East Brazil for FMA in 2005 (non-epidemic year, row 1) and 2008 (epidemic year, row 2). DIR category boundaries defined by 50, 100, 300 and 500 cases per 100,000 inhabitants.

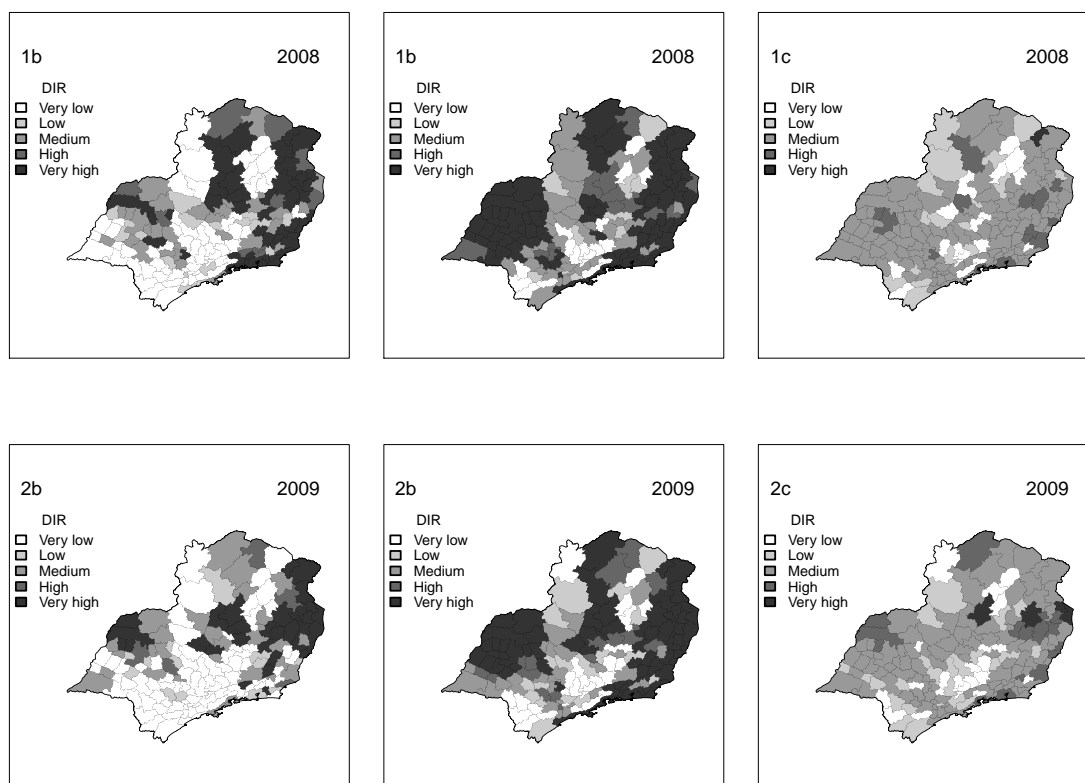


Figure 7. (a) Observed DIR, (b) predicted DIR using GLMM and (c) predicted DIR using current surveillance model (CSM) for FMA season in 2008 (row 1) and 2009 (row 2). Category boundaries defined by 50, 100, 300 and 500 cases per 100,000 inhabitants.

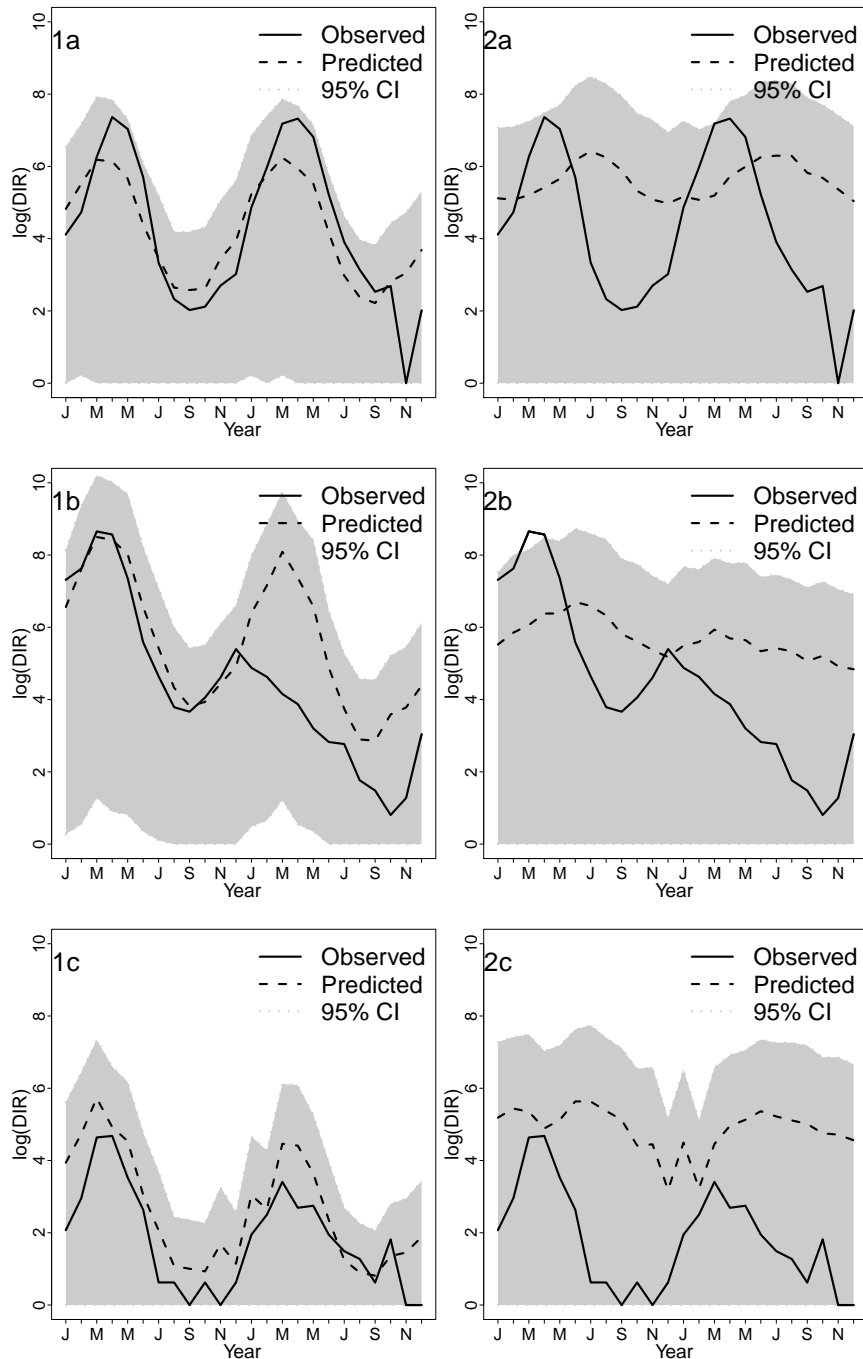


Figure 8. Time series of observed (solid line), posterior predictive mean (dashed line) and 95% credible intervals for posterior predictive distribution of $\log(\text{DIR})$ from January 2008 - December 2009 using GLMM (column 1) and CSM (column 2) for selected microregions: (a) Belo Horizonte, (b) Rio de Janeiro and (c) São Jose dos Campos.

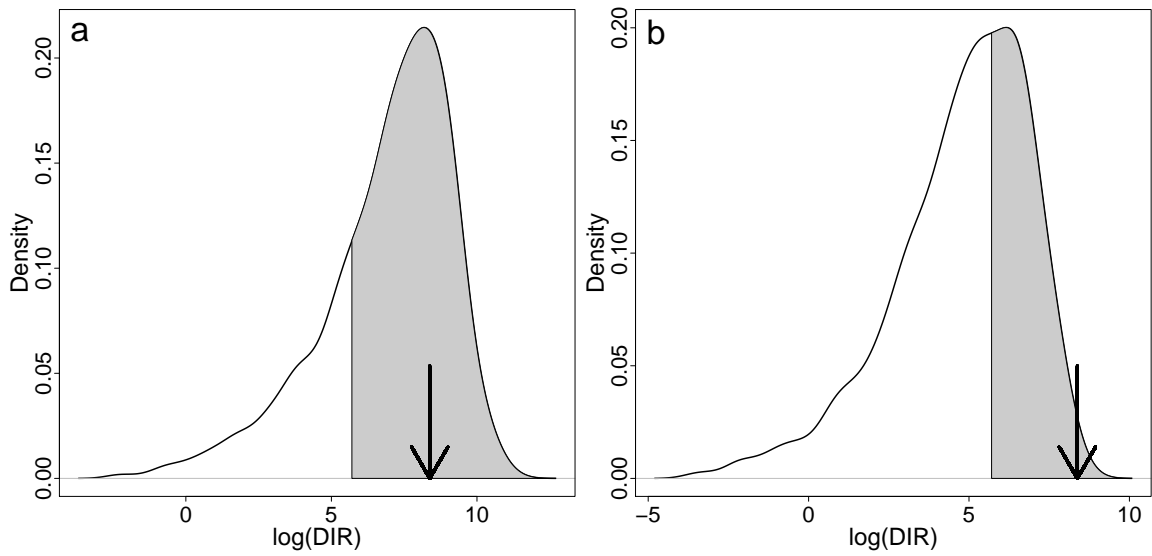


Figure 9. Posterior predictive distributions and probability of exceeding the pre-defined epidemic threshold of 300 cases per 100,000 inhabitants (shaded area) for the microregion Rio de Janeiro, FMA 2008 using (a) GLMM ($p(\text{DIR}) > 300 = 0.75$) and (b) CSM ($p(\text{DIR}) > 300 = 0.37$). Arrow indicates observed DIR.

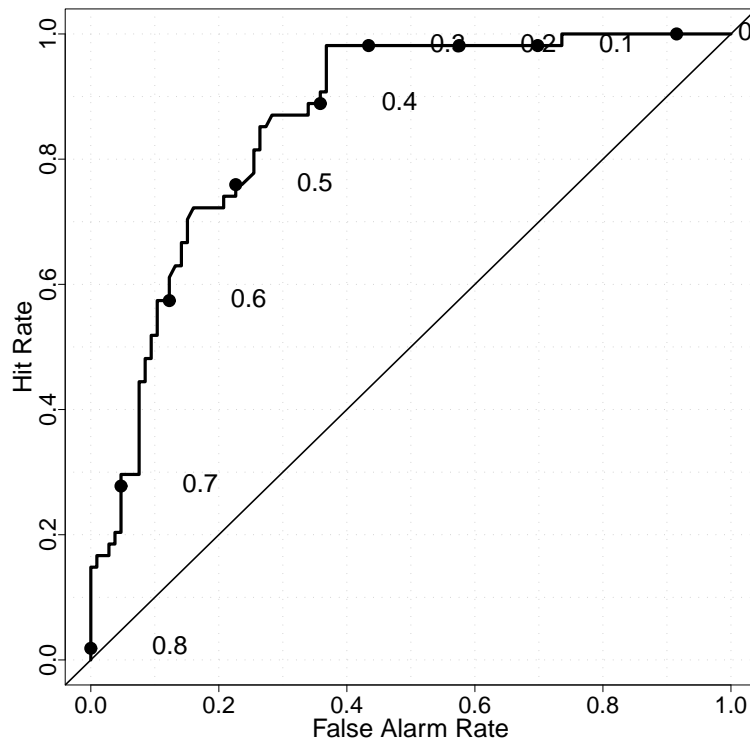


Figure 10. ROC curve for binary event of observed DIR exceeding the epidemic threshold of 300 cases per 100,000 inhabitants for FMA 2008 using GLMM (AUC=0.86).

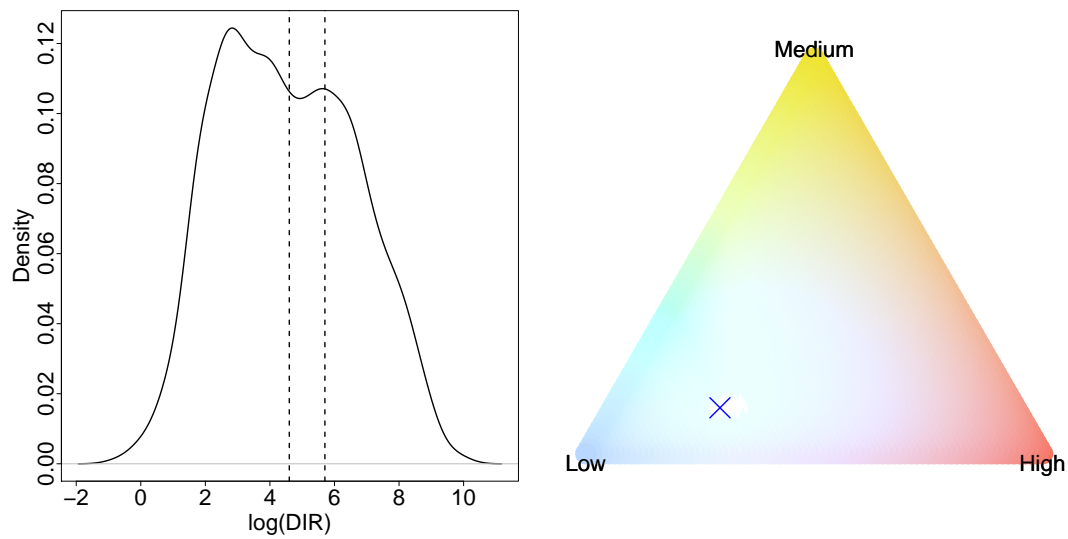


Figure 11. Kernel density of FMA DIR in South East Brazil 2001-2007 with pre-defined category boundaries (dashed lines) of 100 and 300 cases per 100,000 inhabitants (note logarithmic scale) and ternary phase diagram with corners representing ‘Low’ $\mathbf{p} = (1, 0, 0)$, ‘Medium’ $\mathbf{p} = (0, 1, 0)$ and ‘High’ $\mathbf{p} = (0, 0, 1)$ dengue risk. \times marks location of the reference forecast $\mathbf{q} = (0.65, 0.12, 0.23)$.

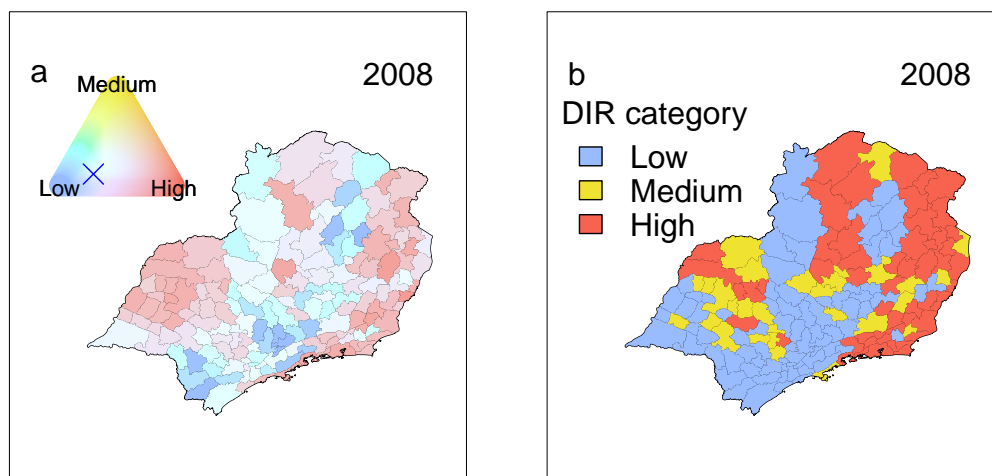


Figure 12. (a) Probabilistic forecast using GLMM and (b) corresponding observed categories for FMA 2008. Category boundaries defined as 100 and 300 cases per 100,000 inhabitants.

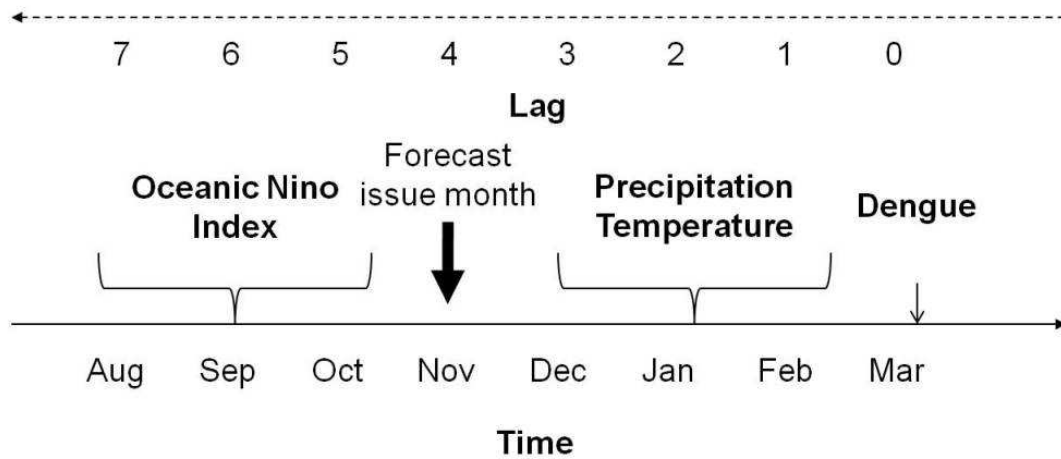


Figure 13. Schematic to show time lags between dengue month of interest (e.g. March), 3-month average precipitation and temperature lagged 2 months prior to dengue month (e.g. December-February) and ONI lagged 6 months prior to dengue month (e.g. August to October, 4 months prior to average precipitation and temperature). A four month lead time could be gained using a forecasting system such as EUROBRISA (<http://eurobrisa.cptec.inpe.br/>).